Influence of drug incorporation strategy on structure and release behavior of alginate beads: A mechanistic study

Wpływ strategii wprowadzania leku na strukturę i zachowanie uwalniania kulek alginianowych: badanie mechanistyczne

Jose Hernandez[1,A–F], Edith Cecilia Rivera-Meza[1,A,D], Adrian de Jesus Rivera-Ramirez[1,A,C], Mercedes Salazar-Hernandez[2,C,E,F], Rosa Hernandez-Soto[1,B,E,F], Alba N. Ardila A.[3,B,C,F]

[1] UPIIG, Instituto Politécnico Nacional, Av. Mineral de Valenciana 200-Interior, Col. Fraccionamiento Industrial Puerto Interior, 3, Silao, Gto., Mexico
[2] Departamento de Ingeniería en Minas, Metalurgia y Geología, División de Ingenierías, Universidad de Guanajuato, Guanajuato, Mexico
[3] Facultad de Ciencias Básicas, Sociales y Humanas, Politécnico Colombiano Jaime Isaza Cadavid, Medellín, Colombia

A – research concept and design; B – collection and/or assembly of data; C – data analysis and interpretation;
D – writing the article; E – critical revision of the article; F – final approval of the article

Polymers in Medicine, ISSN 0370-0747, eISSN 2451-2699 *Polim Med.* 2026;56(1):19–29

Address for correspondence
Jose Hernandez
E-mail: jahernandezma@ipn.mx

Funding sources
None declared

Conflict of interest
None declared

Acknowledgements
The authors wish to thank UPIIG for the infrastructure provided, as well as the Secretaría de Investigación y Posgrado (IPN) and the Laboratorio de Investigación y Caracterización de Minerales y Materiales (LICAMM-UG).

Received on April 7, 2026
Reviewed on May 19, 2026
Accepted on June 19, 2026

Published online on June 30, 2026

Cite as
Hernandez J, Rivera-Meza EC, Rivera-Ramirez AJ, Salazar-Hernandez M, Hernandez-Soto R, Ardila AN. Influence of drug incorporation strategy on structure and release behavior of alginate beads: a mechanistic study. *Polim Med*. 2026;56(1):19–29. doi:10.17219/pim/224828

DOI
10.17219/pim/224828

Abstract

Background. Conventional excipients used in pharmaceutical formulations often exhibit limitations such as uncontrolled drug release and adverse patient responses, highlighting the need for improved drug delivery systems. Sodium alginate beads have been widely investigated as biocompatible carriers due to their ability to form ionically crosslinked hydrogels; however, the influence of drug incorporation strategies on their structural and functional performance remains insufficiently understood. In this study, alginate beads were used as delivery systems for acetylsalicylic acid (ASA) and acetaminophen (AP), comparing encapsulation during gelation with post-synthesis impregnation. The aim was to evaluate how these strategies affect morphology, drug loading, and release mechanisms. Encapsulation resulted in higher drug loading efficiencies (66.5% for AP and 81.8% for ASA) compared to impregnation (61.4% and 73.3%, respectively), as well as a more homogeneous drug distribution within the polymeric matrix. Morphological and structural analyses confirmed that encapsulated beads exhibited more uniform and compact structures, whereas impregnated systems showed heterogeneous drug localization and surface-associated deposits. In vitro release studies revealed that encapsulation promotes controlled and sustained release, while impregnation leads to faster release due to shorter diffusion pathways. Kinetic modeling indicated that AP release follows anomalous transport involving both diffusion and polymer relaxation, whereas ASA release is predominantly diffusion-controlled. These findings demonstrate that the drug incorporation strategy governs the internal structure of alginate beads and directly determines their release behavior, providing mechanistic insight into the rational design of polymeric drug delivery systems with tunable and predictable performance.

Objectives. The main objective of this study was to investigate sodium alginate beads as potential carriers for active pharmaceutical ingredients.

Materials and methods. Sodium alginate beads were prepared by ionotropic gelation and loaded with acetaminophen or acetylsalicylic acid either by encapsulation during gelation or by post-synthesis impregnation. The beads were characterized using FTIR, SEM, and XRD. Drug loading, swelling behavior, in vitro drug release, and release kinetics were also evaluated.

Results. Encapsulation produced beads with higher drug-loading efficiency and more homogeneous structures than impregnation. Consequently, encapsulated systems exhibited more controlled and sustained drug release, whereas impregnated beads showed faster release because of drug localization near the bead surface. Kinetic analysis indicated anomalous transport for acetaminophen and predominantly diffusion-controlled release for acetylsalicylic acid.

Conclusions. This study indicates that the drug incorporation strategy is a key factor governing the structural, functional, and release properties of alginate-based delivery systems.

Streszczenie

Konwencjonalne substancje pomocnicze stosowane w preparatach farmaceutycznych często wykazują ograniczenia, takie jak niekontrolowane uwalnianie leku i niepożądane reakcje pacjentów, co wskazuje na potrzebę ulepszonych systemów dostarczania leków. Kulki alginianu sodu były szeroko badane jako biozgodne nośniki ze względu na ich zdolność do tworzenia jonowo usieciowanych hydrożeli; jednak wpływ strategii wprowadzania leków na ich właściwości strukturalne i funkcjonalne pozostaje nie do końca poznany. W niniejszym badaniu kulki alginianu zastosowano jako systemy dostarczania kwasu acetylosalicylowego (ASA) i acetaminofenu (AP), porównując enkapsulację podczas żelowania i impregnację po syntezie. Celem była ocena wpływu tych strategii na morfologię, nasycenie lekiem i mechanizmy uwalniania. Enkapsulacja skutkowała wyższą wydajnością nasycenia lekiem (66.5% dla AP i 81.8% dla ASA) w porównaniu z impregnacją (odpowiednio 61.4% i 73.3%), a także bardziej jednorodną dystrybucją leku w matrycy polimerowej. Analizy morfologiczne i strukturalne potwierdziły, że otoczone kapsułkami kulki wykazują bardziej jednorodną i zwartą strukturę, podczas gdy systemy impregnowane charakteryzują się heterogeniczną lokalizacją leku i osadami na powierzchni. Badania uwalniania in vitro wykazały, że otoczenie kapsułkami sprzyja kontrolowanemu i przedłużonemu uwalnianiu, podczas gdy impregnacja prowadzi do szybszego uwalniania dzięki krótszym szlakom dyfuzji. Modelowanie kinetyczne wskazało, że uwalnianie AP następuje w wyniku transportu anomalnego, obejmującego zarówno dyfuzję, jak i relaksację polimeru, podczas gdy uwalnianie ASA jest głównie kontrolowane przez dyfuzję. Odkrycia te dowodzą, że strategia wprowadzania leku determinuje strukturę wewnętrzną kulek alginianu i bezpośrednio wpływa na ich zachowanie podczas uwalniania; zapewnia to mechanistyczny wgląd w racjonalne projektowanie polimerycznych systemów dostarczania leków o regulowanej i przewidywalnej wydajności.

Key words: release, mechanism, kinetics, encapsulation, impregnation

Słowa kluczowe: uwalnianie, kinetyka, mechanizm, kapsułkowanie, impregnacja

Introduction

Conventional pharmaceutical formulations frequently exhibit limitations such as uncontrolled drug release, gastrointestinal irritation, and variability in therapeutic response, which are often associated with both the active pharmaceutical ingredients (APIs) and the excipients employed.[1,2] These challenges have driven the development of advanced drug delivery systems capable of improving drug stability, bioavailability, and release control.[3] Among these systems, polymeric matrices based on natural biopolymers have gained significant attention due to their biocompatibility, low toxicity, and versatility.[4–6] In particular, sodium alginate has been extensively studied as a drug delivery material because of its ability to form hydrogels through ionic crosslinking with divalent cations, enabling the encapsulation and controlled release of active compounds.[5,7,8] The physicochemical properties of alginate-based systems, including porosity, swelling behavior,[9] and crosslinking density, are known to strongly influence drug release mechanisms, which may involve diffusion, polymer relaxation, or a combination of both.[8,10]

Despite the extensive literature, the distribution of the drug within the matrix significantly affects release behavior, yet systematic comparative studies on incorporation strategies remain limited, particularly in comparison with studies focused on crosslinking conditions and bead size.[7,8,11,12] However, comparatively less attention has been given to the role of drug incorporation strategies in determining the internal structure of the polymer matrix and its subsequent impact on drug release behavior.[10] The distribution of the drug within the matrix – whether homogeneously embedded or localized near the surface – can significantly affect both loading efficiency and release kinetics.[13] Drug incorporation into alginate matrices can be achieved through different approaches, including encapsulation during gel formation and post-synthesis impregnation.[10] These strategies are expected to produce distinct structural organizations within the beads, influencing drug–polymer interactions and mass transport phenomena.[14] Encapsulation typically promotes uniform drug entrapment within the polymeric network, whereas impregnation often results in heterogeneous distribution and surface localization of the drug.[13] Nevertheless, systematic comparative studies evaluating these approaches under similar experimental conditions remain limited. Despite the extensive use of alginate beads in drug delivery, limited attention has been given to how different drug incorporation strategies influence the internal structure of the matrix and, consequently, the release mechanism. Understanding this relationship is essential for the rational design of controlled release systems. Therefore, the aim of this study is to investigate how different drug incorporation strategies affect the internal structure of alginate beads and their release behavior. The study focuses on elucidating how the incorporation strategy affects bead morphology, drug loading, and release behavior, as well as the underlying transport mechanisms. By establishing structure–function relationships, this work contributes

to the rational design of alginate-based delivery systems with tunable release profiles and improved performance.

Materials and methods

Reagents

All reagents used were of analytical grade, and all aqueous solutions were prepared with deionized water. Calcium chloride ($CaCl_2$, ≥99.9%, Fermont, Monterrey, Nuevo León, México, Productos Químicos Monterrey, S.A. de C.V.), sodium alginate ($NaC_6H_7O_6$, ≥99.9%, Meyer, Ciudad de México, México, Química Suastes S.A. de C.V.), sodium chloride (NaCl, 99%, Meyer, Ciudad de México, México, Química Suastes S.A. de C.V.), hydrochloric acid (HCl, 36%, J.T. Baker, Madrid, Spain, Fisher Scientific S.L.), and sodium hydroxide (NaOH, ≥99.9%, Meyer, Ciudad de México, México, Química Suastes S.A. de C.V.) were employed. Pepsin (from porcine gastric mucosa, CAS 9001-75-6, St. Louis MO, USA, Sigma-Aldrich), acetylsalicylic acid ($C_9H_8O_4$, CAS 50-78-2, Wuppertal, Germany, Bayer), and acetaminophen ($C_8H_9NO_2$, CAS 103-90-2, New Brunswick, Nueva Jersey, USA, Johnson & Johnson) were purchased from Sigma-Aldrich.

Preparation of SAP and API incorporation

Sodium alginate pearls (SAP) were prepared using the ionotropic gelation method. The selected conditions are consistent with widely reported protocols for alginate gelation and bead formation, which strongly influence structural integrity and encapsulation performance.[4,15] The selected alginate concentration, $CaCl_2$ concentration, and processing conditions were chosen based on previous studies reporting their influence on bead formation, encapsulation efficiency, and release behavior. A 4% (w/v) sodium alginate solution ($NaC_6H_7O_6$, 100% purity, Meyer) was maintained under constant stirring at 80°C until a homogeneous viscous solution was obtained. The resulting solution was then pumped dropwise into a 0.2 M calcium chloride solution ($CaCl_2$, Fermont, 100%) maintained at 4°C, as illustrated in Fig. 1.[16] The distance between the $CaCl_2$ solution and the hose (2.5 mm in diameter) was 8 cm while the pumping speed of the sodium alginate solution was 5 mL/min. The droplets immediately formed spherical gel beads due to ionic crosslinking between Ca^{2+} and alginate chains.

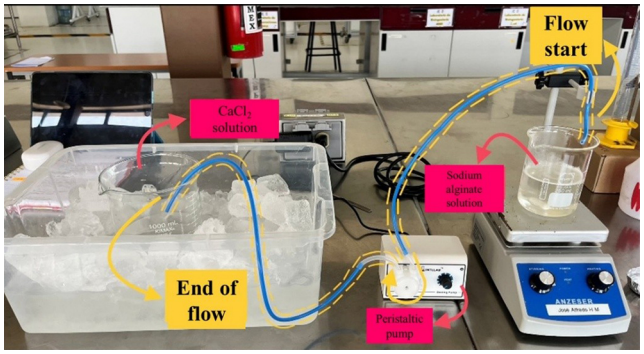

Fig. 1. Constant-flow system for the preparation of sodium alginate beads

The APIs were incorporated into the beads using two different methods: encapsulation and impregnation. These incorporation strategies were selected to evaluate how drug distribution within the polymeric matrix affects structural organization and release mechanisms, as drug localization has been reported to significantly influence mass transport behavior in polymeric systems.[9,10] For encapsulation, the API was mixed directly into the sodium alginate solution before gelation. The resulting mixture was then dropped into a $CaCl_2$ solution to form the beads. For impregnation, SAP were first prepared as blank beads. These preformed beads were then immersed in an API solution and stirred vigorously for 2 h at room temperature to allow diffusion of the active ingredient into the polymeric matrix.[17] The initial mass of API used was 0.5 g while the initial mass of ASA was 0.3 g. After incorporation, the API-loaded beads were stored at 4°C for 24 h to complete hardening, followed by filtration and drying in a convection oven (Memmert, model UNB 100) at 100°C for 1 h. The dried SAP-API were then stored in sealed amber containers under dark conditions to protect them from light exposure and extend their shelf life.

The in vitro release of the APIs was evaluated using a simulated gastric fluid (SGF) prepared according to the composition shown in Table 1. The release conditions were selected to simulate physiological gastric environments and to evaluate the performance of the delivery system under relevant conditions. The SGF was obtained by dissolving the components listed in Table 1 in 1 L of deionized water under vigorous stirring at room temperature. The solution was transferred to an amber glass container with a gas-tight cap and sterilized in an autoclave (Felisa, Zapopan, Jalisco, Mexico) at 121°C and 15 psi for 15 min.[18] Release studies were performed using SGF solutions with and without pancreatin to evaluate the behavior of both encapsulated and impregnated APIs.

A total of 0.3 g of alginate beads was accurately weighed and immersed in 100 mL of simulated gastric fluid within a dissolution apparatus (CROMTEK, Ethik, Santiago, Chile) maintained at 37°C. Aliquots were withdrawn every 10 min to determine the concentration of API. All experiments were performed in triplicate.[16,17] For ASA quantification,

Table 1. Composition of simulated gastric fluid (SGF)[18]

Compound	Weight, g
HCl	16.4*
NaCl	4
Pepsin	10

*mL.

2 mL of each withdrawn sample was mixed in a 1 : 1 : 1 (v/v) ratio with water, sample, and NaOH (1 M), respectively, and the absorbance was measured at 297 nm using a UV–Vis spectrophotometer.[17] For API analysis, aliquots were diluted with 0.1 M HCl and the absorbance was recorded at 300 nm.[18] The release profile of the API was evaluated by calculating the fractional release (M_t/M_∞) as a function of time in the table 2. Experimental data were fitted to various kinetic models commonly used to describe drug release from polymeric systems.[9,19] These models enable the identification of dominant mechanisms such as diffusion, swelling, and polymer relaxation.[8,20] The quality of the fit was assessed using the coefficient of determination (R^2) and the Akaike Information Criterion (AIC) for statistical comparison.[20]All experiments were performed in triplicate, and results are reported as mean ±standard deviation.

Physicochemical and structural characterization of alginate beads loaded with active compounds

X-ray diffraction (XRD) patterns were obtained using a diffractometer (Rigaku Ultima IV) equipped with a Cu Kα radiation source (λ = 1.5418 Å). Data were collected over a 2θ range of 5–80° with a step size of 0.02°. Attenuated total reflectance–Fourier transform infrared spectroscopy (ATR-FTIR) analyses were performed using an infrared spectrometer (Nicolet iS10 Smart, Thermo Scientific) in the range of 4000–550 cm^{-1}, with 32 scans at a resolution of 4 cm^{-1}. Surface morphology and elemental composition were examined using scanning electron microscopy coupled with energy-dispersive X-ray spectroscopy (SEM–EDS) (JEOL JSM-6510 Plus). High-magnification micrographs were acquired to evaluate surface topology and particle size distribution. The size of SAP was determined using a stereomicroscope (Hinotek, model XTD-127) operated at magnifications ranging from ×10 to ×40 under reflected-light illumination. Bead diameters were measured by image analysis using ImageJ software, calculating the equivalent circular diameter of at least 30 beads per sample. Results are reported as mean diameter ± standard deviation. These characterization techniques were employed to correlate structural properties with the incorporation strategy and its impact on drug distribution and release behavior.

Results and Discussion

Effect of the incorporation strategy on bead formation and product yield

The formation of sodium alginate beads is strongly influenced by formulation and processing variables such as alginate concentration, solution viscosity, and gelation conditions. Among these factors, viscosity plays a key role in controlling droplet formation, bead integrity, and reproducibility during ionotropic gelation, since excessively high viscosity hinders solution flow, whereas low viscosity leads to unstable droplet formation and poor bead definition.[4,15,22] During preliminary trials, satisfactory bead formation for AP was achieved using 1% (w/v) sodium alginate, whereas ASA required a higher alginate concentration of 4% (w/v) to obtain stable and well-defined beads. This behavior suggests that the incorporation of each API modifies the physicochemical properties of the precursor solution differently, affecting its processability during gelation. Therefore, alginate concentration was adjusted to ensure adequate bead formation and structural stability for each system.[4,22] The total mass of SAP obtained for each API and incorporation strategy

Table 2. Mathematical models used to describe API release kinetics[9,21]

Models	Equation	Description
Higuchi	$\frac{M_t}{M_\infty} = k_H\sqrt{t}$	k_H is the Higuchi constant that reflects the characteristics of the formulation, M_∞ and M_t are the amounts of drug contained in the pharmaceutical form at the beginning of the release process and the amount of drug released at time *t*.
Power law	$\frac{M_t}{M_\infty} = kt^n$	*k* is the incorporation constant of structural modifications and geometric characteristics of the system (release rate constant), and n is the release exponent (related to the drug release mechanism)
Weibull	$m = 1 - e^{(-\alpha t)}$	*m* is the fraction of drug accumulated in the solution at time *t*. (Drug release profiles of matrix systems)
Peppas-Sahlin	$\frac{M_t}{M_\infty} = k_1 t^m + k_2 t^{2m}$	
	$F = \frac{1}{1 + \frac{k_1}{k_2} t^m}$	Amount of drug released due to the diffusion mechanism (Fickian, F)
	$R = \frac{k_1}{k_2} t^m$	Contribution by swelling or relaxation (R)

is summarized in Table 3. Differences in the recovered mass were observed between APIs and between incorporation methods, indicating that bead formation is affected not only by formulation composition but also by the incorporation strategy. In particular, encapsulation produced higher recovered mass than impregnation for both APIs, which may be associated with a more efficient retention of the drug within the polymeric network during bead formation. These results indicate that the incorporation strategy is not merely a loading step, but a key design parameter that influences bead formation and final product yield. This initial difference is relevant because it anticipates variations in subsequent properties such as morphology, drug distribution, and release performance.

Table 3. Total mass of alginate beads obtained for each API and incorporation strategy

AI	Method	Weight [g]
AP	Encapsulated	14.73 ±0.74
	Impregnated	13.61 ±0.54
ASA	Encapsulated	45.05 ±1.80
	Impregnated	25.84 ±0.78

Physical and functional properties of alginate beads

Morphology

The morphology of alginate beads is a critical factor influencing drug distribution and release behavior. Optical microscopy images of SAP loaded with AP and ASA using encapsulation and impregnation methods are shown in Fig. 2 and 3, respectively. Encapsulated beads exhibited a predominantly spherical morphology with relatively uniform surfaces, indicating stable droplet formation during ionotropic gelation. In contrast, impregnated beads showed partially spherical or irregular geometries, characterized by flattened regions and increased surface roughness. These differences are associated with the absence of drug during bead formation in the impregnation method, which leads to less structural stabilization during gelation.

The more homogeneous morphology observed in encapsulated systems suggests a more uniform internal polymeric network, which may favor controlled diffusion of the drug. Conversely, the irregular structure of impregnated beads indicates heterogeneous drug distribution, likely localized near the surface, which can promote faster release behavior. These observations highlight that the incorporation strategy directly affects the structural organization of the beads and, consequently, their functional performance.[14,23] These morphological differences are consistent with previous reports indicating that drug incorporation methods influence bead structure and surface characteristics, which in turn affect drug release behavior.[24,25]

Size determination

The average diameter of the alginate beads was determined for each API and incorporation method, and the results are presented in Table 4. Encapsulated beads exhibited slightly smaller and more uniform diameters compared to impregnated beads.

$$\mathrm{Dp} = \frac{\sum \text{diameter of each } SAP}{\text{Number of each } SAP} \qquad \text{Eq. (1)}$$

where Dp is the average diameter of the SAP. Table 4 shows the Dp for each pearl.

The differences in size distribution can be attributed to variations in solution viscosity and droplet formation

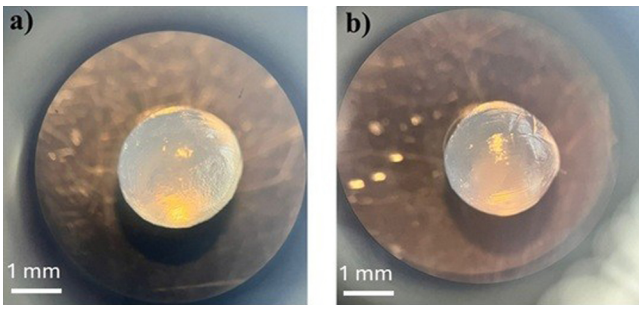

Fig. 2. Optical microscopy images of SAP-AP: (a) Enc and (b) Imp after exposure to SGF. The images illustrate the morphological integrity and surface characteristics of the beads under acidic conditions. Scale bar = 1 mm

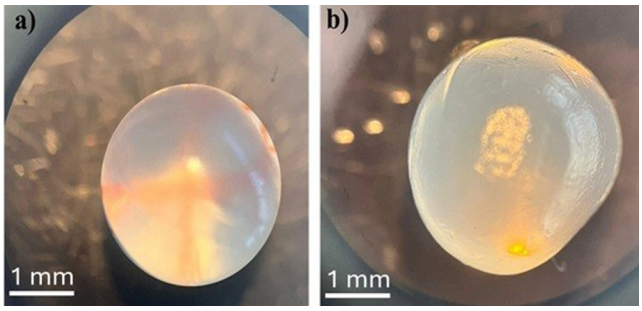

Fig. 3. Optical microscopy images of SAP-ASA: (a) Enc and (b) Imp after exposure to SGF. The images illustrate the morphological integrity and surface characteristics of the beads under acidic conditions. Scale bar = 1 mm.

Table 4. Average and standard deviation for each pearl type

API Method		Dp (mm)
AP	Encapsulated	1.789 ± 0.203
	Impregnated	1.893 ± 0.202
ASA	Encapsulated	2.480 ± 0.224
	Impregnated	2.296 ± 0.226

during gelation. Encapsulation modifies the rheological properties of the alginate solution, leading to more stable droplet formation and reduced size variability. In contrast, impregnation does not influence bead formation directly, resulting in greater variability in bead size.

$$\phi = \frac{4\pi A}{p^2} \qquad \text{Eq. (2)}$$

and

$$R = \frac{4A}{\pi D_{max}^2} \qquad \text{Eq. (3)}$$

where A is the projected area, P is the perimeter and D_{max} is the maximum Feret diameter. A narrower size distribution is generally associated with more predictable drug release profiles, whereas increased variability may lead to heterogeneous release behavior. Therefore, the observed differences in bead size further support the influence of the incorporation strategy on the structural characteristics of the system.

Sphericity and roundness

The sphericity and roundness factors (Table 5) provide quantitative evidence of the morphological differences between encapsulated and impregnated beads. Encapsulated systems exhibited values closer to unity (ϕ ≈ 1), indicating near-spherical particles with uniform geometry. In contrast, impregnated beads showed lower sphericity and roundness values, confirming their irregular morphology. These geometric differences are relevant because particle shape influences surface area, diffusion pathways, and interactions with the dissolution medium. More spherical particles tend to exhibit more controlled and uniform release behavior, whereas irregular particles may facilitate faster release due to increased surface exposure.

Drug content and loading efficiency

The drug content and loading efficiency (Table 6, 7) were significantly influenced by the incorporation strategy. Encapsulation resulted in higher drug loading and improved uniformity compared to impregnation for both APIs.

$$\%\text{API} = \left(\frac{\text{mass of API contained in SAP}}{\text{initial API mass}}\right) \times 100 \qquad \text{Eq. (4)}$$

This behavior can be attributed to the entrapment of the drug within the polymeric network during gelation, which minimizes drug loss and promotes homogeneous distribution. In contrast, impregnation relies on diffusion of the drug into preformed beads, leading to limited penetration and surface accumulation. These findings suggest that the incorporation strategy governs not only the amount of drug incorporated but also its spatial distribution within the matrix, which is expected to play a key role in determining release kinetics.[23,26,27] Taking these results into consideration, the mass balance of the API load in SAP was calculated and is presented in the following table, based on the equation shown below:

$$\%\text{API} = \text{API in SAP} + \text{API in supernatant} + \text{lost API} \qquad \text{Eq. (5)}$$

Moisture content and swelling behavior

The swelling behavior of alginate beads is a key parameter affecting drug release, as it determines water uptake and matrix expansion. The results presented in Table 8 show similar swelling ratios for both incorporation methods, indicating that the polymeric network retains its hydrophilic nature regardless of the strategy used.

$$\%\text{Swelling ratio} = \left(\frac{w_{wet} - w_{dry}}{w_{wet}}\right) \times 100 \qquad \text{eq (7)}$$

where W_{wet}, W_{dry} (g) are the masses of the wet and dry SAP, the values obtained being observed in Table 8. As can be seen, the humidity is similar regardless of the API trapping method used.

However, slight differences in swelling behavior may still influence release kinetics by modifying diffusion pathways

Table 5. SAP sphericity and roundness factor

API Method		φ	R
AP	Encapsulated	0.899	0.912
	Impregnated	0.748	0.774
ASA	Encapsulated	0.938	0.984
	Impregnated	0.660	0.843

Table 6. Yield of SAP obtained from different production methods

AI Method		API, %
AP	Encapsulated	66.50 ±5.38
	Impregnated	61.44 ±4.97
ASA	Encapsulated	81.83 ±6.63
	Impregnated	73.74 ±5.97

Table 7. Mass balance in API load in SAP with different methods

AI Method		SAP-API, g	Supernantant-API, g	Lost API, g
AP	Encapsulated	0.333	0.152	0.015
	Impregnated	0.307	0.138	0.055
ASA	Encapsulated	0.246	0.032	0.022
	Impregnated	0.221	0.041	0.038

Table 8. Moisture content of SAP

AI	Method	Swelling ratio, %
AP	Encapsulated	151.55 ±13.8
	Impregnated	168.57 ±15.3
ASA	Encapsulated	166.15 ±15.1
	Impregnated	177.9 ±16.19

within the hydrogel matrix. These results suggest that, while swelling is primarily governed by polymer properties, the incorporation strategy may indirectly influence water uptake through changes in internal structure.[28–30]

Evaluation of API release from SAP

The in vitro release profiles of AP and ASA from alginate beads prepared by encapsulation and impregnation are presented in Fig. 4. The release behavior differed significantly depending on the incorporation strategy, indicating that drug distribution within the polymeric matrix plays a key role in controlling mass transport. For ASA, encapsulated beads exhibited a more controlled release profile, characterized by a gradual increase in drug release over time. In contrast, impregnated beads showed a faster initial release, indicating that a significant fraction of the drug is located near the bead surface. This behavior is consistent with the expected differences in drug distribution between both incorporation strategies.

Similarly, for AP, impregnated beads exhibited a higher initial release compared to encapsulated systems. Encapsulation reduced the burst effect and promoted a more sustained release, suggesting that the drug is more effectively entrapped within the polymeric network. These results suggest that encapsulation improves control over drug release, whereas impregnation leads to faster release due to surface-localized drug. The differences observed in release behavior can be directly related to the structural characteristics described in the physical and functional properties of alginate beads section. Encapsulated beads exhibited more uniform morphology and internal structure, favoring diffusion-controlled release. In contrast, the heterogeneous structure of impregnated beads facilitates shorter diffusion pathways and faster release kinetics.

Mechanistic analysis of drug release

To elucidate the dominant release mechanisms, experimental data were fitted to several kinetic models commonly used for polymeric systems (Table 9). These models allow differentiation between diffusion-controlled, swelling-controlled, and anomalous transport mechanisms.[8,31] For AP, the Korsmeyer–Peppas and Peppas–Sahlin models provided the best fit, indicating that release is governed by anomalous transport, involving both diffusion and polymer relaxation. This behavior is also consistent with

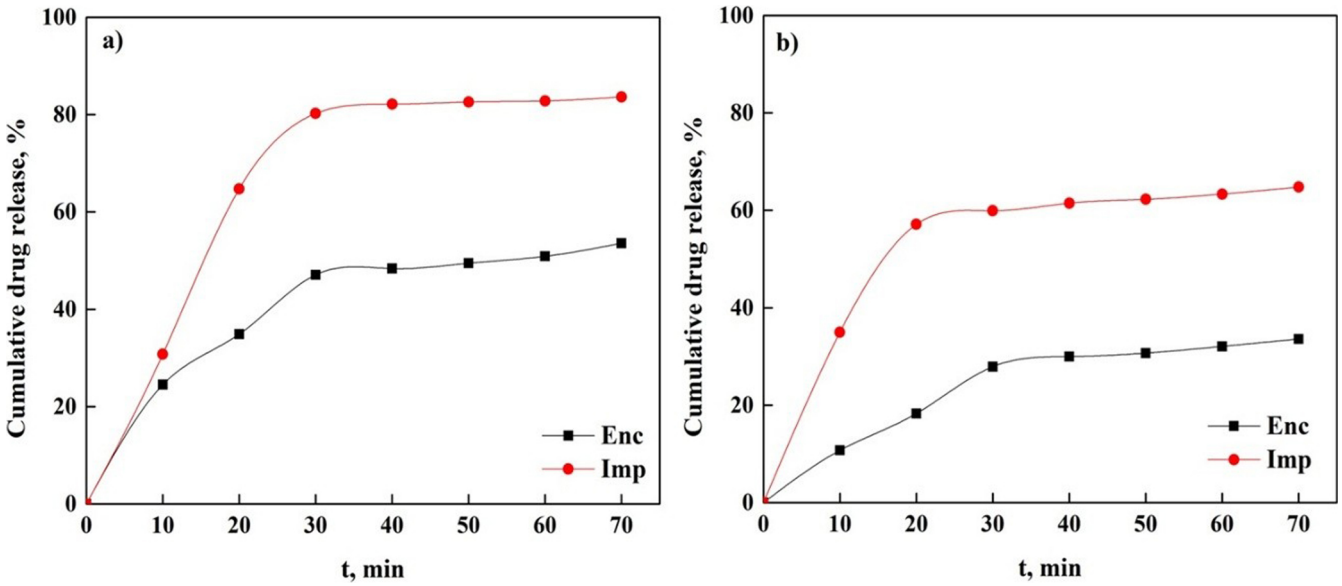

Fig. 4. In vitro release profiles of AP and ASA from alginate beads prepared by encapsulation and impregnation methods

Table 9. Parameters of API release models

Sample	Higuchi			Korsmeyer–Peppas				Peppas–Sahlin					Weibull			
	K_H	R^2	AIC	K	n	R^2	AIC	K_1	K_2	m	R^2	AIC	β	α	R^2	AIC
AP-Enc	4.30	0.96	44.6	0.03	0.66	0.96	−14.8	0.03	0.01	0.43	0.95	−14.6	0.83	0.02	0.95	−12.6
AP-Imp	9.13	0.83	36.3	0.03	0.54	0.95	−17.7	0.03	0.02	0.43	0.95	−17.5	0.65	0.01	0.94	−12.4
ASA-Enc	7.11	0.94	32.2	0.15	0.45	0.97	−1.69	0.16	0.00	0.43	0.80	−1.68	0.61	0.07	0.94	−2.19
ASA-Imp	4.31	0.89	26.6	0.04	0.56	0.94	−9.68	0.04	0.01	0.43	0.83	−9.53	0.61	0.01	0.95	−8.46

drug solubility differences between ASA and AP, which may influence diffusion through the hydrated matrix.

The values of the release exponent ($0.43 < n < 0.85$) suggest that AP release occurs through a combination of Fickian diffusion and matrix relaxation processes. In contrast, the release of ASA was better described by the Weibull model, suggesting a predominantly diffusion-controlled mechanism. The β parameter ($\beta < 1$) indicates an initial rapid release followed by a slower stage, consistent with drug diffusion from a polymeric matrix. The relative contributions of diffusion and polymer relaxation (Table 10) further support these findings. AP release is dominated by polymer relaxation, whereas ASA release is primarily governed by diffusion. These differences may be attributed to the physicochemical properties of each API and their interaction with the alginate matrix.

Importantly, the incorporation strategy significantly influences the dominant release mechanism. Encapsulation promotes a more homogeneous drug distribution within the matrix, leading to diffusion-controlled or mixed transport behavior. In contrast, impregnation results in heterogeneous drug localization and faster release dominated by surface desorption and diffusion. These findings indicate that the incorporation method is a key parameter governing both the kinetics and mechanism of drug release. The results are consistent with established models of drug transport in polymeric systems, where matrix structure and drug distribution determine the dominant release pathways.[9,10] Additionally, differences in drug solubility and molecular size may contribute to the observed variations in transport mechanisms between ASA and AP.

Table 10. Contribution of diffusion and polymer relaxation to API release

AI	Method	F	R
AP	Encapsulated	0.4061	0.5939
	Impregnated	0.7030	0.2970
ASA	Encapsulated	1.0000	0.0000
	Impregnated	0.6920	0.3080

Structural characterization of alginate beads

The structural and physicochemical properties of alginate beads prepared using different incorporation strategies were analyzed by FTIR, SEM, and XRD in order to establish correlations between matrix structure, drug distribution, and release behavior.

FTIR analysis

FTIR spectra of alginate beads before and after drug incorporation are shown in Fig. 5. The spectra exhibit characteristic bands associated with alginate, including broad O–H stretching vibrations (~3200–3400 cm^{-1}), C–H stretching (~2900 cm^{-1}), and asymmetric and symmetric stretching of carboxylate groups (~1600 and ~1400 cm^{-1}), which are responsible for interactions with crosslinking ions. After drug incorporation, slight shifts and changes in band intensity were observed, particularly in the regions associated with hydroxyl and carboxyl groups.[4,32] These variations suggest potential interactions between the APIs and the polymeric matrix, such as hydrogen bonding or electrostatic interactions, which have been widely reported in alginate-based drug delivery systems.[7,13] Encapsulated systems showed more pronounced spectral changes compared to impregnated beads, indicating stronger interactions between the drug and the alginate matrix. In contrast, impregnated systems exhibited minimal spectral modifications, suggesting that the drug is mainly adsorbed on the surface rather than integrated

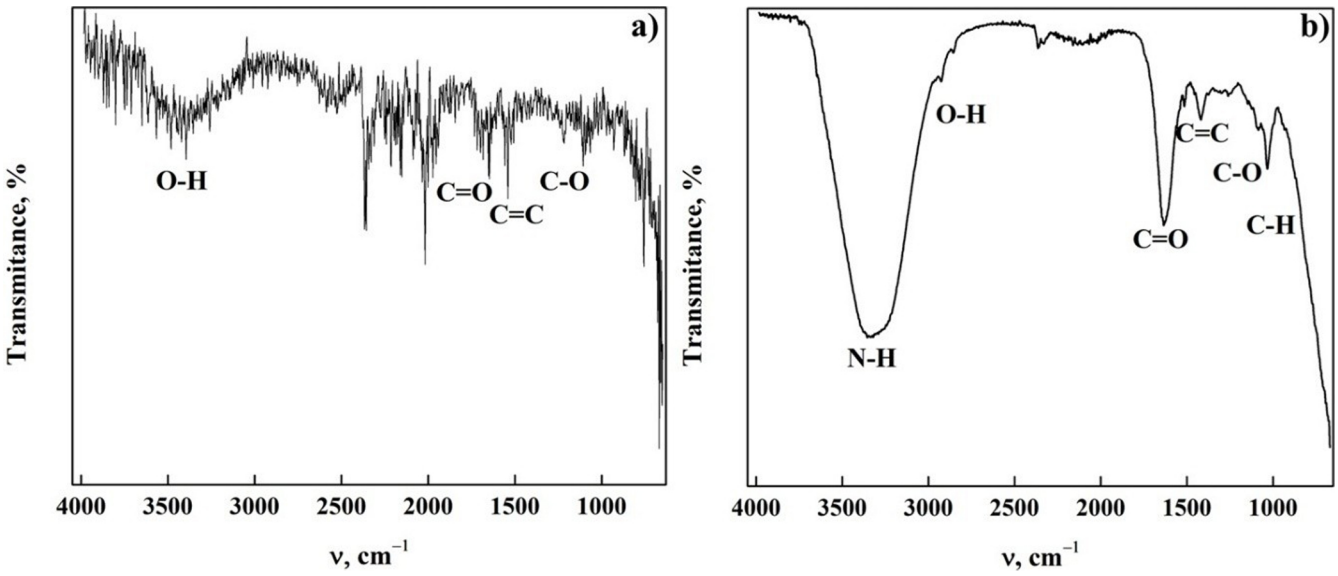

Fig. 5. FTIR spectra of alginate beads before and after drug incorporation using encapsulation and impregnation methods

into the polymer network. These findings support the hypothesis that encapsulation leads to a more homogeneous distribution of the drug within the matrix, whereas impregnation results in surface-localized drug, which is consistent with the release behavior observed in in the evaluation of API release from SAP section. These characteristic bands are consistent with those reported for alginate-based systems in previous studies.[4,31,32]

SEM analysis

SEM images of alginate beads before and after drug incorporation are presented in Fig. 6. Encapsulated beads exhibited a relatively compact and homogeneous internal structure, whereas impregnated beads showed a more heterogeneous morphology with visible surface irregularities. After drug loading, encapsulated systems maintained their structural integrity, indicating that the drug is incorporated within the matrix without significantly altering the external morphology. In contrast, impregnated beads displayed surface deposits and irregularities, which can be attributed to drug accumulation on or near the surface. These morphological differences are directly related to the observed release behavior. Surface-localized drug in impregnated beads facilitates rapid dissolution and faster release, whereas the more uniform structure of encapsulated systems promotes controlled diffusion through the polymeric network.[15] Similar morphological changes associated with drug incorporation and surface deposition have been reported in alginate-based delivery systems, where surface-associated drug leads to faster release behavior compared to matrix-embedded systems.[14,33,34]

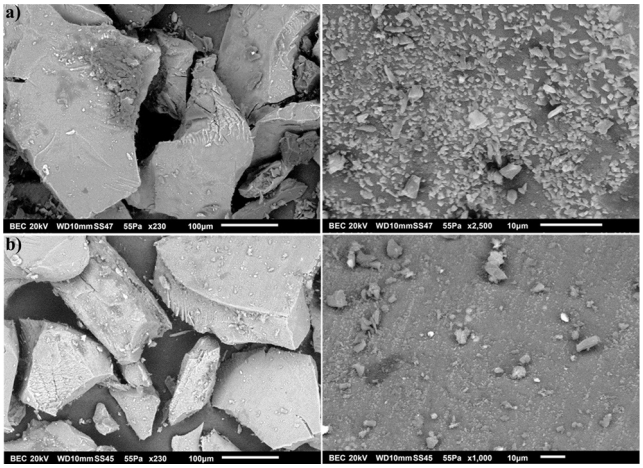

Fig. 6. SEM images of alginate beads prepared by encapsulation and impregnation before and after drug loading

XRD analysis

XRD patterns of alginate beads are shown in Fig. 7. The diffractograms exhibit broad peaks characteristic of amorphous materials. This amorphous behavior is characteristic of alginate-based hydrogels, which typically lack long-range crystalline order due to their ionically crosslinked structure.[4,35] No major changes in crystallinity were observed after drug incorporation, although minor variations in peak intensity were detected in impregnated samples, which may be associated with partial surface crystallization. This behavior is consistent with molecular-level dispersion. The absence of distinct crystalline peaks indicates that the APIs are molecularly dispersed within the polymeric matrix rather than forming separate crystalline phases.[36–38] The absence of sharp crystalline peaks in encapsulated systems further supports the hypothesis of homogeneous drug distribution, whereas any minor changes observed in impregnated samples may be associated with partial surface crystallization of the drug. Overall, the XRD results suggest that

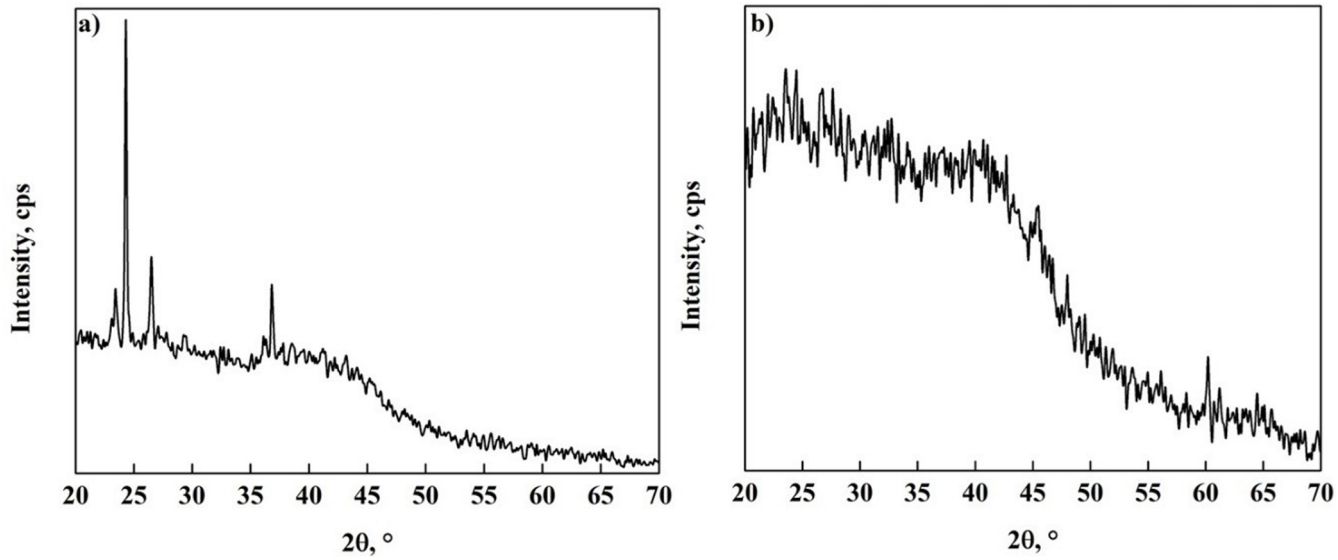

Fig. 7. XRD patterns of alginate beads prepared under different incorporation strategies

the structure of alginate beads is predominantly amorphous, which favors diffusion-controlled drug release.

The results obtained from FTIR, SEM, and XRD analyses consistently indicate that the drug incorporation method significantly alters the internal structure of the alginate matrix. This structural modification is directly related to the observed differences in drug release behavior, where encapsulation promotes a more homogeneous distribution and controlled release, while impregnation leads to surface localization and faster release profiles.

Conclusions

This study indicates that the drug incorporation strategy is a key factor governing the structural, functional, and release properties of alginate-based delivery systems. The comparison between encapsulation and impregnation methods revealed significant differences in bead morphology, drug loading, and release behavior. Encapsulation resulted in more homogeneous structures, higher drug loading efficiency, and improved control over drug release, indicating effective integration of the APIs within the polymeric network. In contrast, impregnation led to heterogeneous drug distribution, with a significant fraction of the drug localized near the bead surface, resulting in faster release profiles. Kinetic modeling showed that AP release is governed by anomalous transport involving both diffusion and polymer relaxation, whereas ASA release is predominantly diffusion-controlled. These differences are directly related to the internal structure of the beads and the spatial distribution of the drug, which are determined by the incorporation strategy. Structural characterization by FTIR, SEM, and XRD supported these findings, confirming that encapsulation promotes a more uniform internal organization, while impregnation leads to surface-associated drug distribution. The consistency between structural analysis and release behavior highlights a clear structure–function relationship in alginate systems. Overall, this work provides mechanistic insight into how drug incorporation strategies influence polymeric delivery systems, demonstrating that the incorporation method is not merely a processing step but a critical design parameter. These findings contribute to the rational design of alginate-based carriers with tunable release profiles and potential applications in controlled drug delivery.

Data Availability Statement

Not applicable.

ORCID iDs

Jose Hernandez 0000-0002-0584-3715
Mercedes Salazar-Hernandez 0000-0001-8480-8725
Rosa Hernandez-Soto Rosa 0000-0001-7053-8808
Alba N. Ardila A. Alba 0000-0002-7675-0647

References

1. Adepu S, Ramakrishna S. Controlled drug delivery systems: Current status and future directions. *Molecules*. 2021;26(19):5905. doi:10.3390/molecules26195905
2. Rouaz K, Chiclana-Rodríguez B, Nardi-Ricart A, et al. Excipients in the Paediatric Population: A Review. *Pharmaceutics*. 2021;13(3):387. doi:10.3390/pharmaceutics13030387
3. Taylor KMG, Aulton ME, eds. *Aulton's Pharmaceutics E-Book: The Design and Manufacture of Medicines*. 5th ed. Elsevier; 2017. ISBN: 978-0-7020-7005-1, 978-0-7020-7001-3.
4. Lee KY, Mooney DJ. Alginate: Properties and biomedical applications. *Prog Polym Sci*. 2012;37(1):106–126. doi:10.1016/j.progpolymsci.2011.06.003
5. Abourehab MAS, Rajendran RR, Singh A, et al. Alginate as a promising biopolymer in drug delivery and wound healing: A review of the state-of-the-art. *Int J Mol Sci*. 2022;23(16):9035. doi:10.3390/ijms23169035
6. Weng Y, Yang G, Li Y, et al. Alginate-based materials for enzyme encapsulation. *Adv Colloid Interface Sci*. 2023;318:102957. doi:10.1016/j.cis.2023.102957
7. Gunjal VB, Sonawane DS, Ahire SK, et al. A review on novel excipients. *Int J Pharm Sci*. 2023;1(9):304-320. doi:10.5281/zenodo.8344687
8. Peppas NA, Bures P, Leobandung W, Ichikawa H. Hydrogels in pharmaceutical formulations. *Eur J Pharm Biopharm*. 2000;50(1):27–46. doi:10.1016/s0939-6411(00)00090-4
9. Siepmann J, Peppas NA. Modeling of drug release from delivery systems based on hydroxypropyl methylcellulose (HPMC). *Adv Drug Deliv Rev*. 2001;48(2–3):139–157. doi:10.1016/s0169-409x(01)00112-0
10. Brazel CS, Peppas NA. Modeling of drug release from swellable polymers. *Eur J Pharm Biopharm*. 2000;49(1):47–58. doi:10.1016/s0939-6411(99)00058-2
11. Paul DR. Elaborations on the Higuchi model for drug delivery. *Int J Pharm*. 2011;418(1):13–17. doi:10.1016/j.ijpharm.2010.10.037
12. Kalkumbe MA, Waghmare S, Kamble H. Microencapsulation: A review. *Int Res J Modern Eng Technol Sci*. 2022;4(5):3844–3850. doi:10.56726/IRJMETS26546
13. Huang X, Brazel CS. On the importance and mechanisms of burst release in matrix-controlled drug delivery systems. *J Control Release*. 2001;73(2–3):121–136. doi:10.1016/s0168-3659(01)00248-6
14. Siepmann J, Siepmann F. Modeling of diffusion controlled drug delivery. *J Control Release*. 2012;161(2):351–362. doi:10.1016/j.jconrel.2011.10.006
15. Smrdel P, Bogataj M, Podlogar F, et al. Characterization of calcium alginate beads containing structurally similar drugs. *Drug Dev Ind Pharm*. 2006;32(5):623–633. doi:10.1080/03639040600599863
16. Jyothi NVN, Prasanna PM, Sakarkar SN, Prabha KS, Ramaiah PS, Srawan GY. Microencapsulation techniques, factors influencing encapsulation efficiency. *J Microencapsul*. 2010;27(3):187–197. doi:10.3109/02652040903131301
17. Kučuk N, Primožič M, Knez Ž, Leitgeb M. Alginate beads with encapsulated bioactive substances from *Mangifera indica* peels as promising peroral delivery systems. *Foods*. 2024;13(15):2404. doi:10.3390/foods13152404
18. Ong CKS, Lirk P, Tan CH, Seymour RA. An evidence-based update on nonsteroidal anti-inflammatory drugs. *Clin Med Res*. 2007;5(1):19-34. doi:10.3121/cmr.2007.698
19. Siepmann J, Peppas NA. Higuchi equation: Derivation, applications, use and misuse. *Int J Pharm*. 2011;418(1):6–12. doi:10.1016/j.ijpharm.2011.03.051
20. Bruschi ML. *Strategies to Modify the Drug Release from Pharmaceutical Systems*. Elsevier/Woodhead Publishing; 2015. ISBN:978-0-08-100092-2.
21. Kosmidis K, Argyrakis P, Macheras P. Fractal kinetics in drug release from finite fractal matrices. *J Chem Phys*. 2003;119(12):6373–6377. doi:10.1063/1.1603731
22. Kalogeropoulou F, Papailiou D, Protopapa C, et al. Design and development of low- and medium-viscosity alginate beads loaded with pluronic® F-127 nanomicelles. *Materials (Basel)*. 2023;16(13):4715. doi:10.3390/ma16134715
23. Sıçramaz H, Dönmez AB, Güven B, Ünal D, Aşbay E. Microstructure and release behavior of alginate–Natural hydrocolloid composites: A comparative study. *Polymers (Basel)*. 2025;17(4):531. doi:10.3390/polym17040531

24. Del Gaudio P, Colombo P, Colombo G, Russo P, Sonvico F. Mechanisms of formation and disintegration of alginate beads obtained by prilling. *Int J Pharm*. 2005;302(1–2):1–9. doi:10.1016/j.ijpharm.2005.05.041
25. Tavakol M, Vasheghani-Farahani E, Hashemi-Najafabadi S. The effect of polymer and $CaCl_2$ concentrations on the sulfasalazine release from alginate-N,O-carboxymethyl chitosan beads. *Prog Biomater*. 2013;2(1):10. doi:10.1186/2194-0517-2-10
26. Szekalska M, Wróblewska M, Czajkowska-Kośnik A, et al. The spray-dried alginate/gelatin microparticles with luliconazole as muco-adhesive drug delivery system. *Materials (Basel)*. 2023;16(1):403. doi:10.3390/ma16010403
27. Azad AK, Al-Mahmood SMA, Chatterjee B, Wan Sulaiman WMA, Elsayed TM, Doolaanea AA. Encapsulation of black seed oil in alginate beads as a pH-sensitive carrier for intestine-targeted drug delivery: In vitro, in vivo and ex vivo study. *Pharmaceutics*. 2020;12(3):219. doi:10.3390/pharmaceutics12030219
28. Kowalski G, Witczak M, Kuterasiński Ł. Structure effects on swelling properties of hydrogels based on sodium alginate and acrylic polymers. *Molecules*. 2024;29(9):1937. doi:10.3390/molecules29091937
29. Das MK, Senapati PC. Furosemide-loaded alginate microspheres prepared by ionic cross-linking technique: Morphology and release characteristics. *Indian J Pharm Sci*. 2008;70(1):77–84. doi:10.4103/0250-474X.40336
30. Bajpai SK, Kirar N. Swelling and drug release behavior of calcium alginate/poly (sodium acrylate) hydrogel beads. *Designed Monomers and Polymers*. 2016;19(1):89–98. doi:10.1080/15685551.2015.1092016
31. Dash S, Murthy PN, Nath L, Chowdhury P. Kinetic modeling on drug release from controlled drug delivery systems. *Acta Pol Pharm*. 2010;67(3):217–223. PMID:20524422.
32. Sriamornsak P, Thirawong N, Korkerd K. Swelling, erosion and release behavior of alginate-based matrix tablets. *Eur J Pharm Biopharm*. 2007;66(3):435–450. doi:10.1016/j.ejpb.2006.12.003
33. Van Haaren C, De Bock M, Kazarian SG. Advances in ATR-FTIR spectroscopic imaging for the analysis of tablet dissolution and drug release. *Molecules*. 2023;28(12):4705. doi:10.3390/molecules28124705
34. Witzler M, Vermeeren S, Kolevatov RO, et al. Evaluating release kinetics from alginate beads coated with polyelectrolyte layers for sustained drug delivery. *ACS Appl Biomater*. 2021;4(9):6719–6731. doi:10.1021/acsabm.1c00417
35. Khajuria DK, Vasireddi R, Priydarshi MK, Mahapatra DR. Ionic diffusion and drug release behavior of core–shell-functionalized alginate–chitosan-based hydrogel. *ACS Omega*. 2020;5(1):758–765. doi:10.1021/acsomega.9b03464
36. Ciarleglio G, Cinti F, Toto E, Santonicola MG. Synthesis and characterization of alginate gel beads with embedded zeolite structures as carriers of hydrophobic curcumin. *Gels*. 2023;9(9):714. doi:10.3390/gels9090714
37. Zhang F. Melt-Extruded Eudragit® FS-based granules for colonic drug delivery. *AAPS PharmSciTech*. 2016;17(1):56–67. doi:10.1208/s12249-015-0357-2
38. Unagolla JM, Jayasuriya AC. Drug transport mechanisms and in vitro release kinetics of vancomycin encapsulated chitosan-alginate polyelectrolyte microparticles as a controlled drug delivery system. *Eur J Pharm Sci*. 2018;114:199–209. doi:10.1016/j.ejps.2017.12.012